52nd IEEE Conference on Decision and Control
December 10-13, 2013. Florence, Italy

Further Results on Distributed Secondary Control in Microgrids

Hedi Bouattour, John W. Simpson-Porco, Florian Dörfler, and Francesco Bullo

Abstract— **This work presents several analysis and design results for primary droop control and secondary control in inductive microgrids. Building on our recent work, we study the problem of set point design in droop-controlled microgrids, and provide a choice of droop coefficients leading to the desired power flows. We then compare and contrast two distributed secondary controllers, and extend them to the case where only a fraction of inverters cooperate in regulating the network frequency. We show that both these secondary-control schemes achieve frequency regulation in the presence of resistive losses.**

I. Introduction

Microgrids are low-voltage electrical distribution networks, heterogeneously composed of distributed generation, storage, load, and managed autonomously from the larger primary network. Microgrids are able to connect to the wide area electric power system through a "Point of Common Coupling", but are also able to "island" themselves and operate independently [1], [2]. Energy generation within a microgrid can be highly heterogeneous, including photovoltaics, wind, geothermal, micro-turbines, etc. Many of these sources generate either variable frequency AC power or DC power, and are interfaced with a synchronous AC grid via power electronic DC/AC *inverters*. In islanded operation, it is through these inverters that actions must be taken to ensure synchronization, security, power balance and load sharing [3].

The so-called primary *droop* controllers have been used successfully to achieve these tasks, see [3]–[9]. For inductive lines, the controller balances the active power injections in the network by instantaneously changing the frequency ω_i of the voltage signal at the i^{th} inverter according to

$$\omega_i = \omega^* - n_i(P_{\mathrm{e},i} - P_i^*)\,, \tag{1}$$

where ω^* is the rated frequency, $P_{\mathrm{e},i}$ is the active electrical power injection at node i, and P_i^* is a nominal active power injection. The parameter $n_i > 0$ is referred to as the *droop coefficient*. Despite forming the foundation for the operation of parallel inverters, droop-controlled networks of inverters and loads have only recently been subject to a rigorous nonlinear analysis. In [10], the authors presented a necessary and sufficient condition for the existence of a unique and locally exponentially stable steady state of a droop-controlled network. Moreover, a secondary-control scheme was devised — termed the *distributed-averaging PI* control — which dynamically regulates the network frequency to its nominal value while maintaining a proportional sharing of power among the inverters. These results are foundational to the present work, and are reviewed in Section II.

In the literature, conservative stability conditions are presented in [11] for all-to-all inverter networks under droop-like controllers. In [12] state feedback is combined with a decentralized LMI strategy to ensure stabilization and frequency regulation, while [13] studies the performance of centralized and decentralized secondary controllers based on integral action. In [14] a distributed secondary-control scheme based on all-to-all inverter frequency averaging is proposed. In [15] a related distributed secondary-control scheme averaging the inverter power outputs is proposed. These variations on the theme of secondary control share the common disadvantage that the steady-state power injections are distorted by the frequency regulation. Unless the controller gains are carefully tuned to the network parameters and the current operating point, the additional integral action disrupts any fair sharing of power between the distributed generators established by the primary stabilizing controller.

The contributions and contents of this work are as follows. Starting from our previous analysis in [10] (reviewed in Section II), we present several novel analysis and design results for frequency-droop and secondary control in inductive microgrids. Section III characterizes the set of droop coefficients which leads to a desired configuration of power flows for primary-controlled networks. Section IV-A presents necessary and sufficient stability conditions for the secondary-control schemes proposed in [14], [15]. Section IV-B partially extends our secondary control results to lossy networks. Section IV-C extends our secondary-control results to the case where only a fraction of inverters participate in frequency regulation. Finally, Section V contains simulations illustrating some of our results. The two distributed secondary control strategies analyzed in this paper have been implemented in an experimental test setup. We refer to [14], [16] for further details. We omit proofs and lengthy algebraic manipulations in this paper and refer the reader to [17] and a forthcoming publication. The remainder of this section recalls some preliminaries and introduces some notation.

Preliminaries and Notation

Vectors and matrices: Given a finite set $\mathcal{V}$, let $|\mathcal{V}|$ denote its cardinality. Given a finite index set $\mathcal{I}$ and a real valued one-dimensional array $\{x_1,\dots,x_{|\mathcal{I}|}\}$, the associated vector is $x \in \mathbb{R}^{|\mathcal{I}|}$ and the associated diagonal matrix is $\mathrm{diag}(\{x_i\}_{i\in\mathcal{I}}) \in \mathbb{R}^{|\mathcal{I}|\times|\mathcal{I}|}$. We denote the $n\times n$ identity matrix by I_n. Let $\mathbf{1}_n$ and $\mathbf{0}_n$ be the n-dimensional vectors of unit and zero entries, and let $\mathbf{1}_n^\perp \triangleq \{x \in \mathbb{R}^n \,:\, \mathbf{1}_n^T x = 0\}$.

Algebraic graph theory: We denote by $G(\mathcal{V},\mathcal{E},A)$ an undirected and weighted graph, where $\mathcal{V}$ is the set of nodes,

This work was supported in part by the National Science Foundation NSF CNS-1135819 and by the National Science and Engineering Research Council of Canada.

Hedi Bouattour, J. W. Simpson-Porco, F. Dörfler and F. Bullo are with the Center for Control, Dynamical Systems and Computation, University of California at Santa Barbara. Email: hebouattour@gmail.com, {johnwsimpsonporco, dorfler,bullo}@engineering.ucsb.edu.

978-1-4673-5716-6/13/$31.00 ©2013 IEEE

$\mathcal{E} \subseteq \mathcal{V} \times \mathcal{V}$ is the set of edges, and $A = A^T \in \mathbb{R}^{|\mathcal{V}|\times|\mathcal{V}|}$ is the *adjacency matrix*. If a number $\ell \in \{1, \ldots, |\mathcal{E}|\}$ and an arbitrary direction is assigned to each edge $\{i,j\} \in \mathcal{E}$, the *node-edge incidence matrix* $B \in \mathbb{R}^{|\mathcal{V}|\times|\mathcal{E}|}$ is defined component-wise as $B_{k\ell} = 1$ if node k is the sink node of edge ℓ and as $B_{k\ell} = -1$ if node k is the source node of edge ℓ, with all other elements being zero. If $\mathcal{A} \triangleq \operatorname{diag}(\{a_{ij}\}_{\{i,j\}\in\mathcal{E}}) \in \mathbb{R}^{|\mathcal{E}|\times|\mathcal{E}|}$ is the diagonal matrix of edge weights, then the positive semidefinite *Laplacian matrix* is given by $L \triangleq B\mathcal{A}B^T$. If the graph is connected, then $\ker(B^T) = \ker(L) = \operatorname{span}(\mathbf{1}_{|\mathcal{V}|})$. For acyclic graphs, $\ker(B) = \emptyset$. In this case, for every $x \in \mathbf{1}_{|\mathcal{V}|}^{\perp}$, that is, $\sum_{i\in\mathcal{V}} x_i = 0$, there exists a unique $\xi \in \mathbb{R}^{|\mathcal{E}|}$ satisfying Kirchoff's Current Law (KCL) $x = B\xi$ [18], [19]. In a circuit, the vector x is interpreted as vector of nodal current injections, and ξ are the associated current flows along edges. We denote by $B^{\dagger} \triangleq (B^TB)^{-1}B^T$ the left inverse of B.

Geometry on the n-torus: The set $\mathbb{S}^1$ is the *unit circle*, an *angle* is a point $\theta \in \mathbb{S}^1$, an *arc* is a connected subset of $\mathbb{S}^1$, and the *n-torus* is $\mathbb{T}^n = \mathbb{S}^1 \times \cdots \times \mathbb{S}^1$. We let $|\theta_1 - \theta_2|$ denote the *geodesic distance* between two angles $\theta_1, \theta_2 \in \mathbb{S}^1$. For $\gamma \in [0, \pi/2[$ and a given graph $G(\mathcal{V}, \mathcal{E}, \cdot)$, let $\Delta_G(\gamma) = \{\theta \in \mathbb{T}^{|\mathcal{V}|} : \max_{\{i,j\}\in\mathcal{E}} |\theta_i - \theta_j| \leq \gamma\}$ be the closed set of angle arrays $\theta = (\theta_1, \ldots, \theta_n)$ with neighboring angles θ_i and θ_j, $\{i,j\} \in \mathcal{E}$ no further than γ apart.

II. MICROGRIDS, DROOP CONTROL AND DAPI CONTROL

A. Droop-controlled inverters in islanded microgrids

We model a microgrid as a linear AC circuit with purely inductive admittance matrix $Y \in j\mathbb{R}^{n\times n}$. The associated connected, undirected, and complex-weighted graph is $G(\mathcal{V}, \mathcal{E}, A)$ with node set (or buses) $\mathcal{V} = \{1, \ldots, n\}$, edge set (or branches) $\mathcal{E} \subset \mathcal{V} \times \mathcal{V}$, and symmetric edge weights (or admittances) $a_{ij} = -Y_{ij} = -Y_{ji} \in \mathbb{C}$ for every branch $\{i,j\} \in \mathcal{E}$, where Y is the bus admittance matrix. Within this paper we restrict ourselves to the acyclic (or "radial") topologies prevalent in low voltage distribution networks. We partition the set of buses as $\mathcal{V} = \mathcal{V}_L \cup \mathcal{V}_I$, corresponding to the loads and inverters. For simplicity, we denote the respective sizes by $n = |\mathcal{V}|$, $n_L = |\mathcal{V}_L|$, and $n_I = |\mathcal{V}_I|$.

To each node $i \in \mathcal{V}$, we associate the voltage phasor $V_i = E_i e^{\sqrt{-1}\theta_i}$ corresponding to the magnitude $E_i > 0$ and the phase angle $\theta_i \in \mathbb{S}$ of a harmonic voltage solution to the AC circuit equations with nominal frequency ω^*. The active power injection $P_{\mathrm{e},i} \in \mathbb{R}$ at node $i \in \mathcal{V}$ is then given by [20]

$$P_{\mathrm{e},i}(\theta) = \sum\nolimits_{j=1}^{n} E_iE_j|Y_{ij}|\sin(\theta_i - \theta_j)\,. \tag{2}$$

Each load $i \in \mathcal{V}_L$ demands a constant amount of active power $P_i^* \leq 0$ and satisfies the power balance equation

$$0 = P_i^* - P_{\mathrm{e},i}(\theta)\,, \quad i \in \mathcal{V}_L\,. \tag{3}$$

The frequency of each inverter is controlled according to the droop control law (1). Since the deviation of the inverter frequency from the nominal network frequency equals the instantaneous change of the phase angle, i.e., $\dot{\theta}_i = \omega_i - \omega^*$, the droop control (1) can be equivalently rewritten as

$$D_i\dot{\theta}_i = P_i^* - P_{\mathrm{e},i}(\theta) + u_i(t)\,, \quad i \in \mathcal{V}_I\,, \tag{4}$$

where $D_i \triangleq n_i^{-1}$ is the (inverse) droop coefficient, $u_i : \mathbb{R}_{\geq 0} \to \mathbb{R}$ is a secondary control input, and $P_i^* \in [0, \overline{P}_i]$ is a nominal injection setpoint, where $\overline{P}_i$ is the rating (power limit) of inverter i. Within this article, we assume that all voltage magnitudes E_i are constant. It can be shown [10], [21] that our results are robust to unmodeled voltage dynamics, which we illustrate in simulations in Section V.

B. Stability, Synchronization, and Power Sharing

Within this subsection, we consider the droop-controlled microgrid (3)-(4) in the absence of secondary control: $u_i = 0$ for all $i \in \mathcal{V}_I$. If the system (3)-(4) possesses a frequency-synchronized solution $\dot{\theta}_i(t) = \omega_{\mathrm{sync}} \in \mathbb{R}$ for all $i \in \{1, \ldots, n\}$, then a summation over all equations (3)-(4) yields the synchronization frequency ω_{sync} as the *scaled power imbalance*

$$\omega_{\mathrm{sync}} \triangleq \frac{\sum_{j\in\mathcal{V}} P_j^*}{\sum_{j\in\mathcal{V}_I} D_j}\,. \tag{5}$$

By transforming to a rotating coordinate frame $\theta(t) \mapsto \theta(t) - \omega_{\mathrm{sync}}t \pmod{2\pi}$, a frequency-synchronized solution of (3)-(4) is equivalent to an equilibrium of the system

$$0 = \widetilde{P}_i - P_{e,i}(\theta)\,, \qquad i \in \mathcal{V}_L\,, \tag{6a}$$

$$D_i\dot{\theta}_i = \widetilde{P}_i - P_{e,i}(\theta)\,, \qquad i \in \mathcal{V}_I\,, \tag{6b}$$

where $\widetilde{P}_i = P_i^*$ for $i \in \mathcal{V}_L$, and $\widetilde{P}_i = P_i^* - D_i\omega_{\mathrm{sync}}$ for $i \in \mathcal{V}_I$. Notice that the scaled injections $\widetilde{P}$ are balanced, $\mathbf{1}_n^T\widetilde{P} = 0$, and the equations (6) feature an inherent rotational symmetry, that is, they are invariant under a rotation of all angles by the same amount. The following result gives the necessary and sufficient condition for the existence of a stable equilibrium of (6), or equivalently, a synchronized solution of the droop-controlled microgrid (3)-(4) [10, Theorem 2].

Theorem 2.1: **(Existence and Stability of Sync'd Solution).** Consider the droop-controlled microgrid (3)-(4) without secondary-control input $u_i = 0$ for all $i \in \mathcal{V}_I$. Assume that the network G is acyclic, and let $\xi \in \mathbb{R}^{|\mathcal{E}|}$ be the unique vector of edge power flows satisfying KCL, given by $\xi = B^{\dagger}\widetilde{P}$. The following two statements are equivalent:

(i) **Synchronization:** there exists an arc length $\gamma \in [0, \pi/2[$ such that the closed-loop system (3)-(4) possesses a locally exponentially stable and unique (modulo rotational symmetry) synchronized solution $t \mapsto \theta^*(t) \in \Delta_G(\gamma)$ for all $t \geq 0$; and

(ii) **Flow Feasibility:** the power flow is feasible, i.e.,

$$\Gamma \triangleq \|\mathcal{A}^{-1}\xi\|_{\infty} < 1\,. \tag{7}$$

If the equivalent statements (i) and (ii) hold true, then the quantities $\Gamma \in [0, 1[$ and $\gamma \in [0, \pi/2[$ are related uniquely via $\Gamma = \sin(\gamma)$, and the synchronized solution $\theta^*(t) \in \Delta_G(\gamma)$ satisfies $\dot{\theta}^*(t) = \omega_{\mathrm{sync}}\mathbf{1}_n$ and $\mathbf{sin}(B^T\theta^*(t)) = \mathcal{A}\xi$.

While Theorem 2.1 gives the necessary and sufficient condition for the existence of a synchronized solution to the closed-loop system (3)-(4), it offers no immediate guidance on how to select the control parameters P_i^* and D_i to satisfy the actuation constraint $P_{\mathrm{e},i} \in [0, \overline{P}_i]$. The following definition gives the proper criteria for this selection.

Definition 1: **(Proportional Droop Coefficients).** The droop coefficients are selected proportionally if for all $i, j \in \mathcal{V}_I$

$$P_i^*/D_i = P_j^*/D_j \text{ and } P_i^*/\overline{P}_i = P_j^*/\overline{P}_j \,. \tag{8}$$

This proportional choice of droop gains leads to a fair power sharing among the inverters according to their ratings and subject to their actuation constraints [10, Theorem 7].

Theorem 2.2: **(Power Flow Constraints and Power Sharing).** Consider a synchronized solution of the droop-controlled microgrid (3)-(4) without secondary-control input ($u_i = 0$ for all $i \in \mathcal{V}_I$), and let the droop coefficients be selected proportionally. Define the total load $P_L \triangleq \sum_{i\in\mathcal{V}_L} P_i^*$. The following two statements are equivalent:

(i) **Injection Constraints:** $0 \leq P_{\mathrm{e},i} \leq \overline{P}_i, \;\; \forall i \in \mathcal{V}_I$;

(ii) **Load Constraint:** $0 \leq -P_L \leq \sum_{j\in\mathcal{V}_I} \overline{P}_j$.

Moreover, the inverters share the total load P_L proportionally according to their power ratings, that is, $P_{\mathrm{e},i}/\overline{P}_i = P_{\mathrm{e},j}/\overline{P}_j$, for each $i, j \in \mathcal{V}_I$.

C. Distributed Averaging PI Control

From Theorem 2.1, the droop controller (4) assures that the closed loop (3)-(4) (with $u_i = 0$) synchronizes to the constant frequency ω_{sync} given by (5). The purpose of the secondary control $u_i(t)$ in (4) is to regulate the synchronization frequency to its nominal value $\omega_{\text{sync}} = 0$. Equivalently, the secondary-control input needs to transform the droop-controlled system (3)-(4) into the rotating frame (6a)-(6b).

Together with the primary proportional droop controller (4), the following distributed averaging proportional integral (DAPI) controller has been proposed by the authors [10]:

$$\boxed{u_i = -p_i \;,\; k_i\dot{p}_i = D_i\dot{\theta}_i + \sum_{j\in\mathcal{V}_I} L_{\mathrm{c},ij}\left(\frac{p_i}{D_i} - \frac{p_j}{D_j}\right).} \tag{9}$$

Here, L_{c} is the Laplacian matrix of a connected communication graph G_{c} between the inverters, $p_i \in \mathbb{R}$ is an auxiliary power variable and $k_i > 0$ is a gain, for each $i \in \mathcal{V}_I$. The resulting closed-loop system is then given by

$$0 = P_i^* - P_{\mathrm{e},i}(\theta)\,, \qquad i \in \mathcal{V}_L\,, \tag{10a}$$

$$D_i\dot{\theta}_i = P_i^* - p_i - P_{\mathrm{e},i}(\theta)\,, \qquad i \in \mathcal{V}_I\,, \tag{10b}$$

$$k_i\dot{p}_i = D_i\dot{\theta}_i + \sum_{j\in\mathcal{V}_I} L_{\mathrm{c},ij}\left(\frac{p_i}{D_i} - \frac{p_j}{D_j}\right), \qquad i \in \mathcal{V}_I\,. \tag{10c}$$

The following result summarizes the stability of the closed-loop system (10) for an acyclic network [10, Theorem 8].

Theorem 2.3: **(Stability of DAPI-Controlled Network).** Consider an acyclic network of droop-controlled inverters and loads in which the inverters can communicate through the communication graph G_c, as described by the closed-loop system (10) with parameters $k_i > 0$, $P_i^* \in [0, \overline{P}_i]$, and $D_i > 0$ for $i \in \mathcal{V}_I$, and connected Laplacian $L_{\mathrm{c}} \in \mathbb{R}^{n_I\times n_I}$. The following two statements are equivalent:

(i) **Stability of Primary Droop Control:** the droop control stability condition (7) holds; and

(ii) **Stability of DAPI Control:** there exists an arc length $\gamma \in [0, \pi/2[$ such that the system (10) possesses a locally exponentially stable and unique (modulo rotational symmetry) equilibrium $\big(\theta^*, p^*\big) \in \Delta_G(\gamma)\times\mathbb{R}^{n_I}$.

If the equivalent statements (i) and (ii) hold true, then the unique (modulo symmetry) equilibrium $\theta^* \in \mathbb{T}^n$ is given as in Theorem 2.1 (ii), along with $p_i^* = D_i\omega_{\text{sync}}$ for $i \in \mathcal{V}_I$.

As a result of Theorem 2.3, the unique equilibrium of the primary-controlled system is recovered. As a consequence, if the droop coefficients are selected proportionally, then the DAPI controller (9) preserves the proportional power sharing property of the primary droop controller.

III. Power Flow Design Using Droop Coefficients

The proportional choice (8) of droop coefficients results in proportional power sharing and determines all droop coefficients up to a positive constant. In this section we address the following "controllability" question: how much can one influence the steady-state injections of the inverters (or the steady-state branch flows of the network) through the choice of droop coefficients? In particular, given a vector of desired steady-state injections $P_I^{\text{set}} \in \mathbb{R}^{n_I}$ for the inverters, when and how can one select the droop coefficients to generate these steady state injections? We make the following standing assumptions in this section.

Assumption 1: **(Primary Control and Actuation).**

(i) **No Secondary Control:** $u_i = 0$ for all $i \in \mathcal{V}_I$;

(ii) **Nominal Injection:** $P_i^* = \overline{P}_i$ for each $i \in \mathcal{V}_I$; and

(iii) **Serviceable Load:** $-\sum_{j\in\mathcal{V}_I}\overline{P}_j < \sum_{j\in\mathcal{V}_L} P_j^* \leq 0$;

From (5), Assumption 1 guarantees that $\omega_{\text{sync}} \neq 0$ (specifically, that $\omega_{\text{sync}} > 0$), and hence that the droop coefficients influence the steady-state inverter power injections $P_{\mathrm{e},i} = P_i^* - \omega_{\text{sync}}D_i$, $i \in \mathcal{V}_I$. One could formulate alternate assumptions such that $\omega_{\text{sync}} < 0$, and all of the following results go through with minor modifications.

Definition 2: **(Power Injection Set-Point).** A vector $P^{\text{set}} \in \mathbb{R}^n$ is a *power injection set-point* if $P^{\text{set}} \in \mathbf{1}_n^\perp$ and $P_i^{\text{set}} = P_i^*$ for $i \in \mathcal{V}_L$.

A power injection set-point is a point of power balance, and the demand at the loads cannot be altered. In what follows, we characterize a feasible power injection set-point.

Definition 3: **($\boldsymbol{\gamma}$-Feasible Set-Point).** Let $P^{\text{set}} = (P_L^*, P_I^{\text{set}})^T$ be a power injection set-point, with $\xi^{\text{set}} \in \mathbb{R}^{|\mathcal{E}|}$ being the associated branch flows $\xi^{\text{set}} = B^\dagger P^{\text{set}}$, and let $\gamma \in [0, \pi/2[$. The power injection set-point P^{set}

(i) satisfies the *nodal actuation constraint* if $P_i^{\text{set}} < \overline{P}_i$, $i \in \mathcal{V}_I$;

(ii) is *$\boldsymbol{\gamma}$-feasible* if it satisfies the nodal actuation constraint and $\|\mathcal{A}^{-1}\xi^{\text{set}}\|_\infty \leq \sin(\gamma)$.

The following result characterizes possible selections of droop coefficients that lead to a desired set-point.

Theorem 3.1: **(Power Injection Set-Point Design).** Let $P^* \in \mathbb{R}^n$ satisfy Assumption 1, let P^{set} be a power injection set-point, and let $\gamma \in [0, \pi/2[$. The following statements are equivalent:

(i) **Coefficient Selection:** there exists a selection of droop coefficients such that the steady-state power injections satisfy $P_{\mathrm{e}}(\theta^*) = P^{\text{set}}$, with $\theta^* \in \Delta_G(\gamma)$; and

(ii) **Set-Point Feasibility:** P^{set} is a γ-feasible power injection set-point.

Moreover, for any $\beta > 0$, the choice of droop coefficients

$$D_i = \beta(\overline{P}_i - P_i^{\text{set}}) > 0\,, \quad i \in \mathcal{V}_I, \tag{11}$$

leads to the desired property of the synchronized steady state.

For inverters operating in parallel, designing P_I^{set} is equivalent to designing the branch flows since $\xi^{\text{set}} = B^\dagger P^{\text{set}} = P_I^{\text{set}}$. For general acyclic graphs, the mapping between nodal injections and branch flows is one-to-one, and the set of designable branch flows is *exactly* the image under $B^\dagger$ of the set of γ-feasible power injection set-points, and no larger.

IV. Extensions of Secondary Control

A. Alternative Distributed Averaging PI Control Scheme

Another secondary distributed PI controller has been presented in [14]. The proposed secondary-control input $u_i(t)$ to the dynamics (3)-(4) is given by an integral feedback‡ of the *weighted average frequency*§ among the inverters:

$$\boxed{u_i(t) = -p_i \quad , \quad k_i \dot{p}_i = \frac{\sum_{j\in\mathcal{V}_I} D_j \dot{\theta}_j}{\sum_{j\in\mathcal{V}_I} D_j}\,,} \tag{12}$$

Here, $p_i \in \mathbb{R}$ is again an auxiliary power variable and $k_i > 0$ is a gain, for each $i \in \mathcal{V}_I$. Notice that, for zero nominal injections $P_i^* = 0$, the weighted average frequency in (12) is the sum of inverter power injections $P_{e,i}(\theta)$ minus the effect of the secondary control. In this case, we recover a control strategy reminiscent of the one advocated in [15].

By explicit numerical counter-examples for asymmetric setups (e.g., non-identical inverters and non-uniform admittances in a parallel topology), it can be shown that the droop-controlled system (3)-(4) with the secondary control (12) fails to achieve power sharing unless the values of k_i are carefully selected. In the following, we suggest the choice

$$k_i = k/D_i\,, \quad i \in \mathcal{V}_I\,, \tag{13}$$

where $k > 0$ is constant. Thus, the integral channels have the time-constants *inverse* to the proportional droop control channels (4). In this case, the closed loop is given by

$$0 = P_i^* - P_{\text{e},i}(\theta)\,, \qquad i \in \mathcal{V}_L\,, \tag{14a}$$

$$D_i\dot{\theta}_i = P_i^* - P_{\text{e},i}(\theta) - p_i\,, \qquad i \in \mathcal{V}_I\,, \tag{14b}$$

$$k\frac{\dot{p}_i}{D_i} = \frac{\sum_{j\in\mathcal{V}_I} D_j\dot{\theta}_j}{\sum_{j\in\mathcal{V}_I} D_j}\,, \qquad i \in \mathcal{V}_I\,. \tag{14c}$$

By changing coordinates $q_i = p_i/D_i - \omega_{\text{sync}}$ for $i \in \mathcal{V}_I$ and observing that $k\dot{q}_i = \frac{\sum_{j\in\mathcal{V}_I} D_j\dot{\theta}_j}{\sum_{j\in\mathcal{V}_I} D_j}$ is identical for all $i \in \mathcal{V}_I$, we can rewrite the closed-loop equations (14) as

$$0 = \widetilde{P}_i - P_{\text{e},i}(\theta)\,, \qquad i \in \mathcal{V}_L\,, \tag{15a}$$

$$D_i\dot{\theta}_i = \widetilde{P}_i - P_{\text{e},i}(\theta) - D_i q\,, \qquad i \in \mathcal{V}_I\,, \tag{15b}$$

$$k\dot{q} = \frac{\sum_{j\in\mathcal{V}_I} D_j\dot{\theta}_j}{\sum_{j\in\mathcal{V}_I} D_j}\,. \tag{15c}$$

Notice that equation (15c) in the transformed system can be implemented as a *centralized integrator*. For these reasons, we refer to the controller (4), (12) with the choice of gains (13) as the centralized averaging proportional integral (CAPI) controller. This perspective is not only insightful and shows the communication complexity of the CAPI controller (12)-(13), but equations (15) are also convenient for the analysis.

Theorem 4.1: **(Stability of CAPI-Controlled Network).** Consider an acyclic network of droop-controlled inverters and loads in which all inverters can communicate and average their frequencies, as described by the closed-loop system (14) with parameters $k > 0$, $P_i^* \in [0, \overline{P}_i]$, and $D_i > 0$ for $i \in \mathcal{V}_I$. The following two statements are equivalent:

(i) **Stability of Primary Droop Control:** the droop control stability condition (7) holds;

(ii) **Stability of CAPI Control:** there exists an arc length $\gamma \in [0, \pi/2[$ such that the system (14) possesses a locally exponentially stable and unique (modulo rotational symmetry) equilibrium $(\theta^*, p^*) \in \Delta_G(\gamma) \times \mathbb{R}^{n_I}$.

If the equivalent statements (i) and (ii) hold true, then the unique (modulo symmetry) equilibrium is given as in Theorem 2.1 (ii), along with $p_i^* = D_i\omega_{\text{sync}}$ for $i \in \mathcal{V}_I$.

Analogous to the DAPI control (9), Theorem 4.1 guarantees that the equilibrium of the primary-controlled system is preserved. Hence, the CAPI control (12) preserves the proportional power sharing for proportional droop coefficients.

B. Extension of secondary control to lossy networks

We now study the operation of the DAPI and CAPI controllers when the network contains line conductances resulting in power losses. The admittance matrix $Y \in \mathbb{C}^{n\times n}$ is now given by $Y = G_{ij} + \sqrt{-1}B_{ij}$, where $G \in \mathbb{R}^{n\times n}$ is the conductance matrix and $B \in \mathbb{R}^{n\times n}$ is the susceptance matrix. The active electrical power $P_{\text{e},i} \in \mathbb{R}$ injected into the network at node $i \in \{1, \dots, n\}$ is then given by [20]

$$P_{\text{e},i}(\theta) = \sum\nolimits_{j=1}^{n} E_i E_j |Y_{ij}| \sin(\theta_i - \theta_j - \phi_{ij})\,, \tag{16}$$

where $|Y_{ij}|^2 = G_{ij}^2 + B_{ij}^2$ and $\phi_{ij} \triangleq -\arctan(G_{ij}/B_{ij})$. In compact vector notation, the frequency droop controller is

$$D\dot{\theta} = P^* - P_e(\theta)\,, \tag{17}$$

where $D = \operatorname{diag}(\mathbf{0}_{|\mathcal{V}_L|}, \{D_i\}_{i\in\mathcal{V}_I})$. The analysis of lossy circuits is considerably more challenging than in the lossless case. Indeed, no concise conditions are known that establish existence, uniqueness, and stability of equilibria for the primary-controlled system (16)-(17). To study secondary control strategies in lossy networks, we assume the existence of a solution to the primary-controlled microgrid (16)-(17).

Assumption 2: **(Existence and uniqueness in presence of losses).** There exists an arc length $\gamma \in [0, \pi/2[$ such that

‡The controller proposed in [14] also contains a proportional feedback of the average frequency. We found that such a proportional feedback destroys the desired proportional power sharing, unless the gains are carefully tuned. For these reasons and since the resulting closed loop is hardly amenable to an analytic investigation, we omit the proportional feedback channel here.

§The controller in [14] contains a true arithmetic average with all $D_i = 1$ in (12). Since the synchronization frequency (5) is obtained by a weighted average and since $D_i\dot{\theta}_i$ is the inverter injection $P_{e,i}(\theta)$ (for $P_i^* = 0$), we found the choice (12) more appealing and intuitive. Simulations suggest that any convex combination of the inverter frequencies yields identical results.

the closed-loop system (16)-(17) possesses a unique (modulo rotational symmetry) and frequency-synchronized solution $\theta^*(t) \in \Delta_G(\gamma)$, with $\dot{\theta}^*(t) = \omega^*_{\text{sync}} \in \mathbb{R}$ for all $t \geq 0$.

By summing over the equations (17) in steady state, we obtain the corresponding unique synchronization frequency

$$\omega^*_{\text{sync}} = \frac{\sum_{i \in \mathcal{V}} P^*_i - \sum_{i \in \mathcal{V}} P_{\text{e},i}(\theta^*)}{\sum_{i \in \mathcal{V}_I} D_i}\,.$$

Under Assumption 2, $\theta^* \in \Delta_G(\gamma)$ is the unique solution to

$$P^* - P_e(\theta) - D\,\frac{\sum_{i \in \mathcal{V}} P^*_i - \sum_{i \in \mathcal{V}} P_{\text{e},i}(\theta)}{\sum_{i \in \mathcal{V}_I} D_i}\mathbf{1}_n = \mathbf{0}_n\,. \quad (18)$$

Theorem 4.2: **(Existence & Uniqueness of Sync'd Solutions for DAPI/CAPI Control systems in Lossy Networks).** If Assumption 2 holds, then the unique (modulo rotational symmetry) synchronized solution for the DAPI-controlled system (10), (16) and the CAPI-control system (14), (16) is given by $(\theta, p) = (\theta^*, D_I \omega^*_{\text{sync}} \mathbf{1}_{n_I}) \in \Delta_G(\gamma) \times \mathbb{R}^{n_I}$.

After having established the existence of equilibria for the secondary control systems, we now study their stability. Simulation studies suggest that local stability is maintained independent of the conductance magnitudes. While it is difficult to find a general stability proof, we can extend the stability from the lossless case using continuity arguments.

Theorem 4.3: **(Stability of Equilibria for DAPI/CAPI Controllers in Lossy Networks).** Let Assumption 2 hold, and let $(\theta^*, D_I \omega^*_{\text{sync}} \mathbf{1}) \in \Delta_G(\gamma) \times \mathbb{R}^{n_I}$, with $\gamma \in [0, \pi/2[$, be the unique synchronized solution of the DAPI-controlled system (10), (16) and of the CAPI-controlled system (14), (16). There exists $\varepsilon > 0$ such that if $\|G\| < \varepsilon$, the equilibrium given by $(\theta^*, D_I \omega^*_{\text{sync}} \mathbf{1})$ is locally exponentially stable.

It turns out that the proportional power sharing properties of the closed loop are maintained in the presence of losses.

Theorem 4.4: **(Power Sharing in Lossy Networks).** Let Assumption 2 hold, and consider a lossy network of droop-controlled inverters and loads (17). If the droop coefficients are selected proportionally as in (8), then the inverters share the total load P_L proportionally according to their power ratings. Moreover, the secondary DAPI and CAPI controllers preserve the power sharing.

C. Partial DAPI/CAPI Control

The DAPI controller (9) requires a connected communication network among the inverters. In presence of communication constraints, it may be desirable that only a subset of inverters participates in regulating the network frequency, see Figure 1. To investigate this scenario, we partition the set of inverters as $\mathcal{V}_{I_P} \cup \mathcal{V}_{I_S} = \mathcal{V}_I$, where the action of the $\mathcal{V}_{I_P}$ inverters is restricted to primary droop control, and the $\mathcal{V}_{I_S}$ inverters perform the secondary DAPI/CAPI control. We assume that at least $|\mathcal{V}_{I_S}| \geq 1$ inverters participate in the secondary CAPI control, respectively, $|\mathcal{V}_{I_S}| \geq 2$ for the DAPI control. As a special case, notice that $|\mathcal{V}_{I_S}| = 1$ inverter performing CAPI control is analogous to AGC (automatic generation control) in transmission networks [20]. Given this partitioning, the inverter control equations become

$$D_i \dot{\theta}_i = P^*_i - P_{\text{e},i}(\theta)\,, \qquad i \in \mathcal{V}_{I_P}\,, \quad (19a)$$

$$D_i \dot{\theta}_i = P^*_i - P_{\text{e},i}(\theta) + u_i(t)\,, \qquad i \in \mathcal{V}_{I_S}\,. \quad (19b)$$

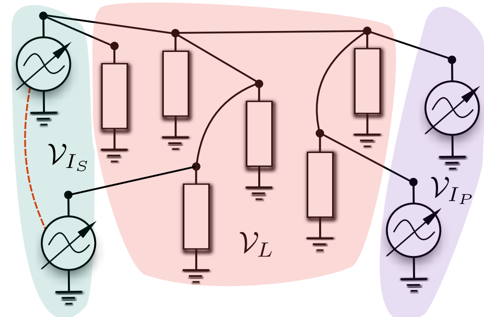

Fig. 1. Schematic illustration of partial secondary control. The red dotted line represents a communication link.

The scaled power imbalance is now defined by

$$\omega^{**}_{\text{sync}} \triangleq \Big(\sum\nolimits_{j \in \mathcal{V}} P^*_j\Big) \Big/ \Big(\sum\nolimits_{j \in \mathcal{V}_{I_S}} D_j\Big)\,. \quad (20)$$

The following result shows that partial secondary control strategies stabilize the network and regulate the frequency.

Theorem 4.5: **(Stability of Partial secondary-controlled Network).** Consider an acyclic network of droop-controlled inverters and loads, as described by the closed-loop system (3), (19), with parameters $P^*_i \in [0, \overline{P}_i]$ and $D_i > 0$ for $i \in \mathcal{V}_I$. The secondary-control input u_i is defined by either (9) (DAPI) or (12) (CAPI) for all $i \in \mathcal{V}_{I_S}$ with $k_i > 0$. The following two statements are equivalent:

(i) **Stability of Primary Droop Control:** the droop control stability condition (7) holds; and

(ii) **Stability of Secondary Control:** there exists an arc length $\gamma \in [0, \pi/2[$ such that the two systems (3), (9), (19) and (3), (12), (19) possess the unique and locally exp. stable equilibrium $\big(\theta^*, p^*\big) \in \Delta_G(\gamma) \times \mathbb{R}^{|\mathcal{V}_{I_S}|}$.

If the equivalent statements (i) and (ii) hold true, then θ^* is given as in Theorem 2.1 with $p^*_i = D_i \omega^{**}_{\text{sync}}$ for $i \in \mathcal{V}_{I_S}$.

In steady-state, the inverters $\mathcal{V}_{I_P}$ are effectively frequency-dependent negative loads, we obtain the following power sharing properties of the partial secondary control schemes.

Theorem 4.6: **(Power Flow Constraints and Power Sharing).** Consider the same setup as in Theorem 4.5, and define the total load by $P_L \triangleq \sum_{i \in \mathcal{V}_L} P^*_i$. If the droop coefficients and the set points of the inverters $i \in \mathcal{V}_{I_S}$ performing secondary control are selected proportionally as in (8), then the following two statements are equivalent:

(i) **Injection Constraints**: $0 \leq P_{e,i}(\theta^*) \leq \overline{P}_i \quad \forall i \in \mathcal{V}_I$;

(ii) **Load and Set-Point Constraints**:

$$\sum\nolimits_{j \in \mathcal{V}_{I_P}} P^*_j \leq -P_L \leq \sum\nolimits_{j \in \mathcal{V}_{I_P}} P^*_j + \sum\nolimits_{j \in \mathcal{V}_{I_S}} \overline{P}_j\,.$$

Moreover, the inverters performing secondary control share the load residual $P_L - \sum_{i \in \mathcal{V}_{I_P}} P^*_i$ proportionally according to their power ratings, i.e., $P_{\text{e},i}/\overline{P}_i = P_{e,j}/\overline{P}_j$ for all $i, j \in \mathcal{V}_{I_S}$.

V. Simulation Study

We illustrate a subset of our results by means of a simulation, where two inverters operating in parallel supply a variable load. Since the DAPI controller (9) is thoroughly covered in [10], we show the robustness and performance of

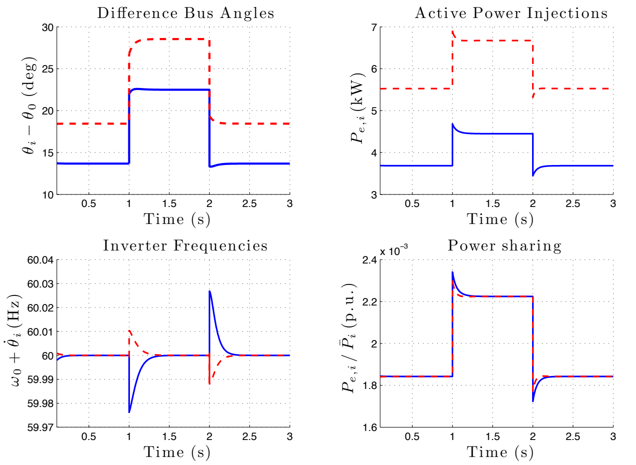

Fig. 2. CAPI-controlled closed loop (14) for two inverters supplying a load. The solid (blue) plots correspond to inverter 1, and the dashed (red) plots correspond to inverter 2. The simulation is initialized at a non-stationary value, and the active and reactive power demand at the load doubles at $t = 1$s and then returns to its original vaue at $t = 2$s.

the CAPI controller (12)-(13). The inverter voltage magnitudes are controlled via the *quadratic voltage-droop* [22]

$$\tau_i \dot{E}_i = -C_i E_i (E_i - E_i^*) - Q_{\mathrm{e},i}, \quad i \in \mathcal{V}_I, , \quad i \in \{1, 2\},$$

where $E_i^* > 0$ is the nominal voltage magnitude, $C_i > 0$ (resp. $\tau_i > 0$) is the proportional (resp. integral) quadratic voltage-droop coefficient, and $Q_{\mathrm{e},i} \in \mathbb{R}$ is the reactive power injection [20]. The simulation parameters are reported in Table I, and a time-domain simulation is shown in Figure 2. Observe that the CAPI controlled system (14) is robust and achieves an acceptable transient performance in presence of lossy lines and unmodeled reactive power and voltage dynamics. One fundamental disadvantage of CAPI controller (12)-(13) over the DAPI controller (9) (besides the communication complexity) is that the time constants of the proportional feedback (4) and the integral feedback (12) are coupled through (13) and cannot be chosen independently if one wishes to achieve power sharing. Whereas our choice of control gains in Table I is certainly not optimal, we found that the droop coefficients of the CAPI controller generally need to be selected smaller (resulting in a more aggressive primary control) than those of the corresponding DAPI controller to achieve an acceptable secondary control performance.

VI. Conclusions

In this work we have presented several extensions of primary and secondary control in microgrids. In particular, we have shown the following: if the primary controller succeeds in stabilizing the network, then the DAPI and CAPI secondary controllers regulate the frequency and preserve the power sharing, even in the presence of losses. A challenging and open problem is the feasibility and stability analysis of microgrids with non-infinitesimal conductances.

TABLE I

Parameter values for simulation in Figure 2.

Parameter	Symbol	Value
Nom. Frequency	$\omega^*/2\pi$	60 Hz
Nom. Voltages	E_i^*	$[120, 122]$ V
Output/Line Induc.	L_i	$[0.7, 0.5]$ mH
Output/Line Resist.	R_i	$[0.14, 0.1]\,\Omega$
Inv. Ratings (P)	$P_i^* = \overline{P}_i$	$[6, 9]$ kW
Load (P)	$P_0^*(t)$	$P_0^* \in \{-2.5, -5\}$kW
Load (Q)	$Q_0^*(t)$	$Q_0^* \in \{-.5, -1\}$kvar
ω–Droop Coeff.	D_i	$[4, 6] \times 10^2$ W · s
Sec. Droop Coeff.	k_i	$[1, 1] \times 10^{-6}$ s
Quadratic E–Droop Coeff.	C_i	$[1, 1.5]$ 10^{-3} s
Quadratic E–Droop Int. Coeff.	τ_i	$[5, 5]$ s

References

[1] Q.-C. Zhong and T. Hornik, *Control of Power Inverters in Renewable Energy and Smart Grid Integration*. Wiley-IEEE Press, 2013.

[2] J. M. Guerrero, J. C. Vasquez, J. Matas, L. G. de Vicuna, and M. Castilla, "Hierarchical control of droop-controlled AC and DC microgrids–a general approach toward standardization," *IEEE Transactions on Industrial Electronics*, vol. 58, no. 1, pp. 158–172, 2011.

[3] J. A. P. Lopes, C. L. Moreira, and A. G. Madureira, "Defining control strategies for microgrids islanded operation," *IEEE Transactions on Power Systems*, vol. 21, no. 2, pp. 916–924, 2006.

[4] M. C. Chandorkar, D. M. Divan, and R. Adapa, "Control of parallel connected inverters in standalone AC supply systems," *IEEE Transactions on Industry Applications*, vol. 29, no. 1, pp. 136–143, 1993.

[5] A. Tuladhar, H. Jin, T. Unger, and K. Mauch, "Parallel operation of single phase inverter modules with no control interconnections," in *Applied Power Electronics Conference and Exposition*, Atlanta, GA, USA, Feb. 1997, pp. 94–100.

[6] S. Barsali, M. Ceraolo, P. Pelacchi, and D. Poli, "Control techniques of dispersed generators to improve the continuity of electricity supply," in *IEEE Power Engineering Society Winter Meeting*, New York, NY, USA, Jan. 2002, pp. 789–794.

[7] R. Majumder, A. Ghosh, G. Ledwich, and F. Zare, "Power system stability and load sharing in distributed generation," in *Power System Technology and IEEE Power India Conference*, New Delhi, India, Oct. 2008, pp. 1–6.

[8] Y. U. Li and C.-N. Kao, "An accurate power control strategy for power-electronics-interfaced distributed generation units operating in a low-voltage multibus microgrid," *IEEE Transactions on Power Electronics*, vol. 24, no. 12, pp. 2977–2988, 2009.

[9] J. M. Guerrero, J. C. Vasquez, J. Matas, M. Castilla, and L. G. de Vicuna, "Control strategy for flexible microgrid based on parallel line-interactive UPS systems," *IEEE Transactions on Industrial Electronics*, vol. 56, no. 3, pp. 726–736, 2009.

[10] J. W. Simpson-Porco, F. Dörfler, and F. Bullo, "Synchronization and power sharing for droop-controlled inverters in islanded microgrids," *Automatica*, vol. 49, no. 9, pp. 2603–2611, 2013.

[11] Z. Wang, M. Xia, and M. D. Lemmon, "Voltage stability of weak power distribution networks with inverter connected sources," in *American Control Conference*, Washington DC, USA, Jun. 2013, submitted.

[12] J. Schiffer, A. Anta, T. D. Trung, J. Raisch, and T. Sezi, "On power sharing and stability in autonomous inverter-based microgrids," in *IEEE Conf. on Decision and Control*, Maui, HI, USA, Dec. 2012, pp. 1105–1110.

[13] M. Andreasson, H. Sandberg, D. V. Dimarogonas, and K. H. Johansson, "Distributed integral action: Stability analysis and frequency control of power systems," in *IEEE Conf. on Decision and Control*, Maui, HI, USA, Dec. 2012, pp. 2077–2083.

[14] Q. Shafiee, J. Guerrero, and J. Vasquez, "Distributed secondary control for islanded microgrids - a novel approach," *IEEE Transactions on Power Electronics*, 2013, to appear.

[15] H. Liang, B. J. Choi, W. Zhuang, and X. Shen, "Stability enhancement of decentralized inverter control through wireless communications in microgrids," *Smart Grid, IEEE Transactions on*, vol. 4, no. 1, pp. 321–331, 2013.

[16] J. W. Simpson-Porco, F. Dörfler, Q. Shafiee, J. M. Guerrero, and F. Bullo, "Stability, power sharing, & distributed secondary control in droop-controlled microgrids," in *IEEE Int. Conf. on Smart Grid Communications*, Vancouver, BC, Canada, Oct. 2013, to appear.

[17] H. Bouattour, "Distributed secondary control in microgrids," Master's thesis, University of Stuttgart, May 2013.

[18] N. Biggs, "Algebraic potential theory on graphs," *Bulletin of the London Mathematical Society*, vol. 29, no. 6, pp. 641–683, 1997.

[19] L. O. Chua, C. A. Desoer, and E. S. Kuh, *Linear and Nonlinear Circuits*. McGraw-Hill, 1987.

[20] P. Kundur, *Power System Stability and Control*. McGraw-Hill, 1994.

[21] F. Dörfler, M. Chertkov, and F. Bullo, "Synchronization in complex oscillator networks and smart grids," *Proceedings of the National Academy of Sciences*, vol. 110, no. 6, pp. 2005–2010, 2013.

[22] J. W. Simpson-Porco, F. Dörfler, and F. Bullo, "Voltage stabilization in microgrids using quadratic droop control," in *IEEE Conf. on Decision and Control*, Florence, Italy, Dec. 2013, to appear.